[redacted] DECLASSIFIED NASA TM X-1096

C65-4237

FREE-FLIGHT MEASUREMENTS OF HEAT TRANSFERRED TO THE APOLLO AFTERBODY WITH AND WITHOUT HEAT SHIELD ABLATION

By Layton Yee

Ames Research Center
Moffett Field, Calif.

GROUP 4
Downgraded at 3 year intervals;
declassified after 12 years

CLASSIFIED DOCUMENT–TITLE UNCLASSIFIED
This material contains information affecting the national defense of the United States within the meaning of the espionage laws, Title 18, U.S.C., Secs. 793 and 794, the transmission or revelation of which in any manner to an unauthorized person is prohibited by law.

NOTICE
This document should not be returned after it has satisfied your requirements. It may be disposed of in accordance with your local security regulations or the appropriate provisions of the Industrial Security Manual for Safe-Guarding Classified Information.

NATIONAL AERONAUTICS AND SPACE ADMINISTRATION

[redacted]

[redacted] DECLASSIFIED

FREE-FLIGHT MEASUREMENTS OF HEAT TRANSFERRED TO THE APOLLO AFTERBODY WITH AND WITHOUT HEAT SHIELD ABLATION*

By Layton Yee
Ames Research Center

SUMMARY

14370

Afterbody heat-transfer rates to Apollo-shaped models at 0° angle of attack were measured in a ballistic range by means of a passive telemetry technique. The measurements were made on small gun-launched models with ablating as well as nonablating nose caps. The measured heat-transfer rates are compared with wind-tunnel and shock-tunnel data obtained on sting-mounted models. Cont.

Author

INTRODUCTION

While literature is readily available on heat transfer to stagnation points of spherically nosed vehicles, comparatively little information is available on heat transfer to afterbodies, such as the conical surface of the Apollo command capsule. Some experimental studies have indeed been made on Apollo afterbody heating, but these measurements were invariably made on models which were supported by stings, whose influence on the flow fields was not determinable. Moreover, it is expected that ablation products from the nose cap might affect the afterbody heat-transfer rates. In the light of these points, then, the present investigations were conducted. The data presented herein are the results of one approach to measuring, in free flight, the afterbody heating rates on Apollo-shaped models with ablating as well as nonablating nose caps. The tests were made in the pilot range of the Hypersonic Free-Flight Branch, Ames Research Center.

SYMBOLS

a	speed of sound, ft/sec
c_p	specific heat at constant pressure, Btu/slug $^{\circ}$F
D	model diameter, ft
H	enthalpy, Btu/slug

*Title, Unclassified.

[redacted]

h	heat-transfer coefficient, Btu/sec ft^2 $^\circ$F
k	thermal conductivity, Btu/sec ft $^\circ$F
M	Mach number, V/a
$\dot{m}$	mass-loss rate due to ablation, slug/ft^2 sec
Pr	Prandtl number, $c_p\mu/k$
p	pressure, lb/ft^2
$\dot{q}$	heat-transfer rate, Btu/ft^2 sec
R	maximum cross-sectional radius of model, ft
Re_D	Reynolds number based on diameter, $\rho_\infty V_\infty D/\mu_\infty$
Re_S	local Reynolds number, $\rho_e V_e S/\mu_e$
S	surface distance measured from stagnation point, ft
St	local Stanton number, $h/c_p\rho_e V_e$
V	velocity, ft/sec
α	angle of attack, deg
ρ	density, slug/ft^3
μ	viscosity, slug/sec ft

Subscripts

b	base conditions
e	edge conditions
s	stagnation conditions
∞	free-stream conditions

APPARATUS

The apparatus used in the present tests was adapted from a passive telemetry system developed and used previously to measure stagnation-point heating rates. The technique, described fully in reference 1, involves the launching of a small saboted model into a ballistic range with a light-gas gun of the

type described in reference 2. As a convenience to the reader, a brief description of the system is included in subsequent paragraphs; and refinements and differences in procedure are noted.

The design of the model is shown in figure 1. The temperature-sensing element of the model is an annular copper-constantan thermocouple formed by the copper ring soft-soldered to the constantan disk. A four-turn copper wire coil is soft-soldered to the constantan disk near its center to form the cold junction and to a point on the copper ring to complete the electrical circuit. Three different nose-cap materials were used: aluminum to measure afterbody heat transfer in the absence of ablation, and two plastic materials, nylon and Lexan, to observe any effect on the afterbody heat transfer due to ablation of the forebody. Although the boron nitride forward of the calorimeter is exposed to the afterbody flow, the boron nitride should not begin to ablate because of its high working temperature (1800° F) and the short test duration (3 milliseconds). Because the annular thermocouple of the model may not be heated uniformly, a simple bench test of a simulated annular thermocouple was devised for determining the actual temperature "read" by the thermocouple; and it was found that an annular thermocouple reads a temperature that is between the highest and the lowest, though not necessarily the average temperature. This characteristic of an annular thermocouple is not important in the present tests because the models flew at essentially 0° angle of attack so that any temperature gradient along the periphery of the thermocouple should be negligible.

The experimental setup is shown schematically in figure 2. The light screen, short-duration spark, and electronic timer are the ubiquitous instrumentation for ballistic ranges. The pickup coil is a 400-turn, centertapped, single-layer coil wound on a 4-inch-diameter fiberglas form. Electrostatic shielding is incorporated in the coil form to minimize spurious electrostatic signals. The pickup coil is critically damped with a 3900 ohm resistor connected between the centertap and one end of the coil. A frequency spectrum analyzer was used for determining experimentally the requirements for critical damping. The frequency response of the damped coil is flat to about 180 kc/sec. The signal from the model is recorded on a differential input oscilloscope triggered from an uprange spark source. Five shadowgraph stations and 12 pickup coils were used to record the data.

As the annular copper-constantan thermocouple is heated during the model's flight, a potential difference exists between the heated junction and the cold junction inside the model. The resulting current flowing through the coil produces a magnetic field the strength of which is proportional to the temperature rise of the hot junction. When the model flies through a pickup coil, the magnetic field surrounding the model induces a voltage on the pickup coil. The amplitude of this signal voltage is related to thermocouple emf, coil configurations, model velocity, and other known conditions of the test. The temperature rise of the hot junction on the model can thus be determined; and from successive measured temperature rises, the heat-transfer rates to the model can be computed. A typical oscilloscope record is shown in figure 3. The disturbances on either side of the signal are caused by the discharges of the spark sources immediately uprange and immediately downrange of the pickup

coil. Procedures for the data reduction as well as the derivations of the necessary equations are discussed in detail in reference 1. Since the geometries of the pickup coil and the model coil are the same as those in reference 1, the equations and curve of reference 1 pertaining to mutual inductance between pickup coil and model coil are valid for the present tests.

TEST CONDITIONS

The tests were all made in room temperature (80° F) air at 50-mm Hg pressure. The models were launched at better than 18,000 ft/sec muzzle velocity and flew with pitching amplitudes of less than 5°. The Reynolds number based on free-stream properties and diameter was nominally 170,000. Temperature measurements were made at velocities between 16,700 and 18,500 ft/sec. Because the velocity of 17,500 ft/sec is common to all the tests, it was used in the data reduction as the comparison velocity. In the actual reentry of the Apollo capsule, the Reynolds number based on diameter and free-stream properties at maximum heating, on undershoot and overshoot entry boundaries, is between 130,000 and 780,000 and velocity between 34,600 and 33,400 ft/sec, depending upon the reentry angle. Since ablation temperature for the plastic cap models is attained within a foot of the muzzle of the gun, it is assumed that steady-state ablation has been established by the time the model reaches the first coil station, about 13-feet downrange of the muzzle.

Because of the low ambient density of the present tests, the shadowgraphs show no flow detail whatsoever. However, a shadowgraph showing some flow details was obtained at higher density in another facility having more sensitive photography. It is reproduced in figure 4. The test conditions are as follows: V_∞ = 19,830 ft/sec, M_∞ = 17.6, Re_D = 506,000, and p_∞ = 100 mm Hg. The afterbody flow is clearly separated. Since the present test conditions give a considerably lower Reynolds number, it is reasonable to assume that the afterbody flow on the present models is also separated.

The models in flight are subjected to both convective and radiative heating, the latter from the air and ablation gases that are heated to a luminous condition in the flow field around the model. However, measurements and calculations have indicated that the level of radiative heating on the afterbody is, at the model scale employed here, about two orders of magnitude smaller than the convective. Hence, the data may properly be analyzed on the assumption that only convective heating is present.

RESULTS AND DISCUSSION

The results of the present tests are tabulated below:

Round	Nose-cap material	Velocity, ft/sec		$\dot{q}_b$, Btu/sec ft^2	$\dot{q}_b/\dot{q}_s$
		First coil	Last coil		
500	2024-T4 Al	17,500	16,600	281	0.035
643	2024-T4 Al	18,230	17,180	274	.034
656	2024-T4 Al	18,000	17,070	236	.029
648	2024-T4 Al	18,120	17,140	213	.026
671	Lexan	17,840	16,670	134	.017
544	Nylon	17,940	16,700	116	.014
644	Nylon	18,550	17,020	115	.014
659	Nylon	18,410	17,090	109	.013
658	Lexan	18,420	17,040	105	.013

Test parameters calculated at 17,500 ft/sec: $M_\infty = 15.3$, $Re_D = 170{,}000$, $H_s = 2\times10^5$ Btu/slug, $\dot{q}_s = 8{,}100$ Btu/sec ft^2

A theoretical cold-wall stagnation-point heat-transfer rate, calculated by the method of reference 3 with the velocity gradient determined by the method of reference 4, was used to normalize the experimental afterbody values for both the nonablating and the ablating models. The experimental heating rates to the afterbody of the aluminum nose-capped models (which are not ablating at these test conditions) lie between 2-1/2 and 3-1/2 percent of the calculated stagnation-point heating rates. The afterbody heating rates to the ablating plastic-nosed models are about half those of the nonablating aluminum-nosed models. The atomic constituents (based on atomic weight) of nylon are: 63.7 percent carbon, 9.7 percent hydrogen, 14.2 percent oxygen, and 12.4 percent nitrogen (based on nylon 6,6); and that for Lexan are: 75.6 percent carbon, 5.5 percent hydrogen, and 18.9 percent oxygen (based on bis-phenol-A). In spite of the differences in atomic constituents of the two plastic materials, no drastic difference in afterbody heating was observed. The ablation rate ($\dot{m}$) for the Lexan models is 0.058 slug/sec ft^2, calculated by the method of reference 5; and that for the nylon models is 0.063 slug/sec ft^2 (see ref. 6). The mass injection parameter ($\dot{m}/\rho_\infty V_\infty$) is 0.022 for the Lexan model and 0.024 for the nylon model. Since the mass injection parameter is usually used as a basis for comparing the efficacy of cooling of material injected into the boundary layer, it is not surprising to find that, in view of the similarity of the mass injection parameters, the heating rates to the two plastic-nosed models are reduced by about the same amount. It should be noted

that the nylon and Lexan nose caps are nonchar[redacted]ing ablators wherein the surface temperatures remained low. No measurements were made using the actual Apollo heat-shield material, which is a charring ablator. Therefore, the effect of ablation on the afterbody heating of the actual Apollo capsule, protected by a charring ablator, might be different from that observed for the present tests.

Convective-heat-transfer data can be correlated on a Stanton number versus Reynolds number plot, as discussed in reference 7. The correlation plot of reference 7 is reproduced in figure 5 with the present data, represented by the flagged symbols, added for comparison. The value of $p_b = 4.7p_\infty$, obtained from reference 8, and local properties, evaluated at the free-shear layer above the afterbody and assuming isentropic expansion and equilibrium flow, were used to determine the Stanton numbers and the Reynolds numbers (Re_S). The present measurements were made at a point on the afterbody $S/R = 1.67$ that is slightly different from the one used to evaluate the other data $S/R = 1.84$, but the comparison is still valid because the flow at these two points should not be significantly different at 0° angle of attack. It can be seen that the present data from the nonablating nose-capped models correlate well with the other data, the bulk of which are from wind-tunnel tests of reference 9 and shock-tunnel tests of reference 10. The remaining data are from unpublished sources. The solid line represents the theory for heat transfer to a flat plate in laminar attached flow according to reference 11. The dashed line represents the average heat transfer from laminar separated flow, which, according to reference 12, is 0.56 of the laminar attached flow values for $Pr = 0.72$. This prediction is in fair agreement with the correlated measurements for this station of the afterbody.

CONCLUSIONS

Measurements of heating rates on small free-flight models indicate that the afterbody heating rates to Apollo models with nonablating nose caps are about 3 percent of the calculated stagnation-point heating rates, and the heating rates to the ablating nose-capped models are about half those of the nonablating nose-capped models. The data from the nonablating nose-capped models correlate well with other data obtained from sting-mounted models when compared on a Stanton number versus Reynolds number basis. Theoretical predictions of heat transfer in two-dimensional separated laminar flow are in fair agreement with the correlated data.

Ames Research Center
National Aeronautics and Space Administration
Moffett Field, Calif., Feb. 2, 1965

REFERENCES

1. Yee, Layton; Bailey, Harry E.; and Woodward, Henry T.: Ballistic Range Measurements of Stagnation-Point Heat Transfer in Air and in Carbon Dioxide at Velocities up to 18,000 Feet Per Second. NASA TN D-777, 1961.

2. Curtis, John S.: An Accelerated Reservoir Light-Gas Gun. NASA TN D-1144, 1962.

3. Fay, J. A.; and Riddell, F. R.: Theory of Stagnation Point Heat Transfer in Dissociated Air. J. Aero. Sci., vol. 25, no. 2, Feb. 1958, pp. 73-85, 121.

4. Boison, J. Christopher; and Curtiss, Howard A.: An Experimental Investigation of Blunt Body Stagnation Point Velocity Gradient. ARS J. vol. 29, no. 2, Feb. 1959, pp. 130-5.

5. Savin, Raymond C.; Gloria, Hermilo R.; and Dahms, Richard G.: The Determination of Ablative Properties of Materials in Free-Flight Ranges. NASA TN D-1330, 1962.

6. Chapman, Andrew J.: An Experimental Investigation of Several Ablation Materials in an Electric-Arc-Heated Air Jet. NASA TN D-1520, 1963.

7. Lee, George: Correlation of Heat-Transfer Data for the Apollo Afterbody at Mach Numbers 8 to 20. NASA TM X-855, 1964.

8. Lee, George; and Sundell, Robert E.: Heat-Transfer and Pressure Distributions on Apollo Models at $M = 13.8$ in an Arc-Heated Wind Tunnel. NASA TM X-1069, 1965.

9. Jones, Robert A.: Experimental Investigation of the Overall Pressure Distribution, Flow Field, and Afterbody Heat Transfer Distribution of an Apollo Reentry Configuration at a Mach Number of 8. NASA TM X-813, 1963.

10. Garberoglio, J. E.; and Ryder, M. O., Jr.: Hypersonic Shock Tunnel Pressure and Heat Transfer Tests of the Apollo Reentry Vehicle for North American Aviation. Rep. AA-1712-Y-2, Cornell Aero. Lab., Inc., Dec. 1962.

11. Eckert, E. R. G.: Survey on Heat Transfer at High Speeds. ARL Rep. 189, 1961.

12. Chapman, Dean R.: A Theoretical Analysis of Heat Transfer in Regions of Separated Flow. NACA TN 3792, 1956.

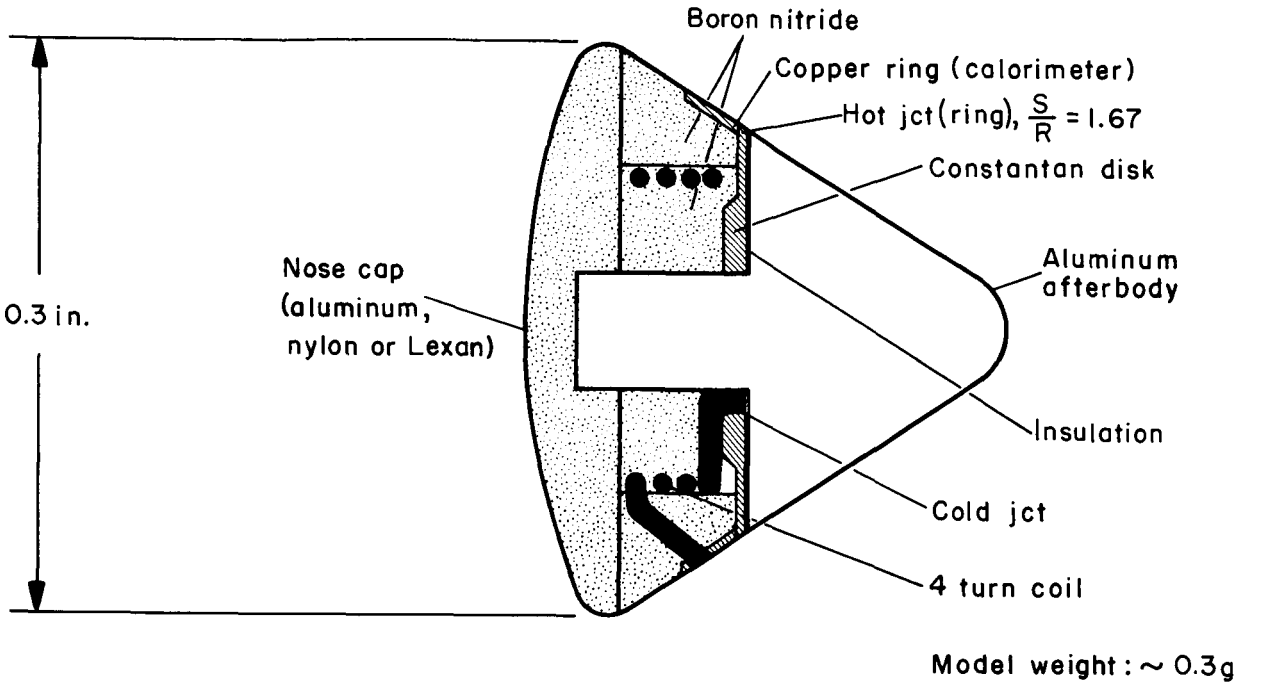

Figure 1.- Passive telemetry model (Apollo reentry capsule).

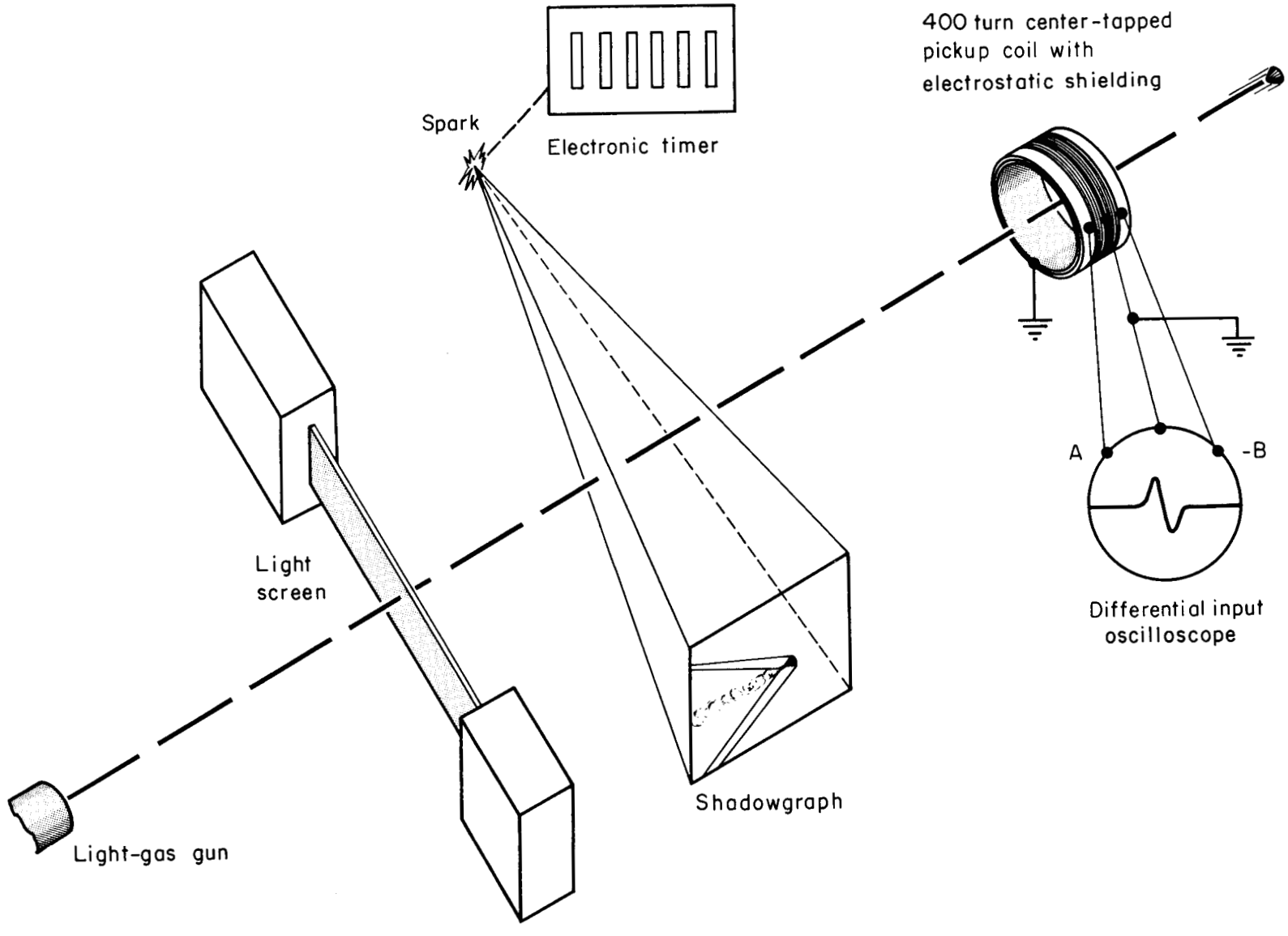

Figure 2.- Experimental setup.

[redacted]

UNCLASSIFIED

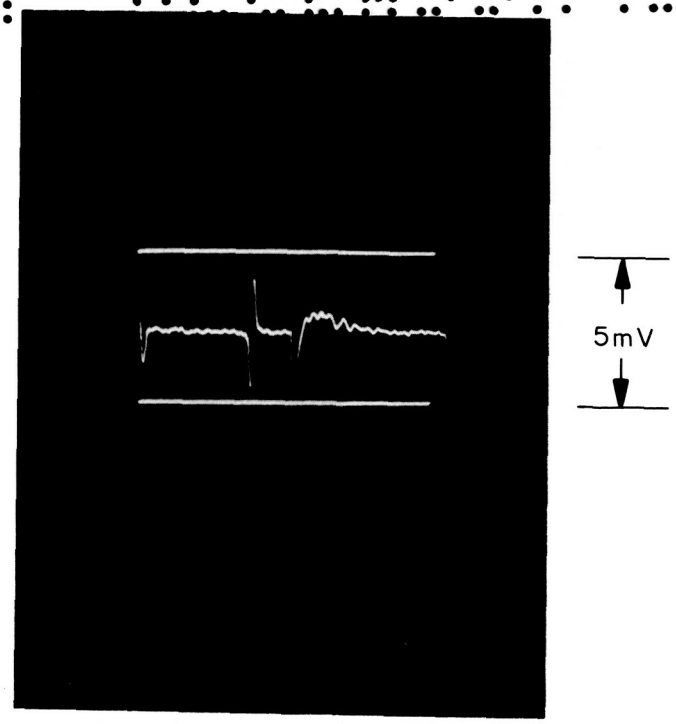

Sweep →

Total sweep time 1 millisecond

Model velocity ≈ 17,500 fps

Figure 3.- Typical oscilloscope record.

[redacted]

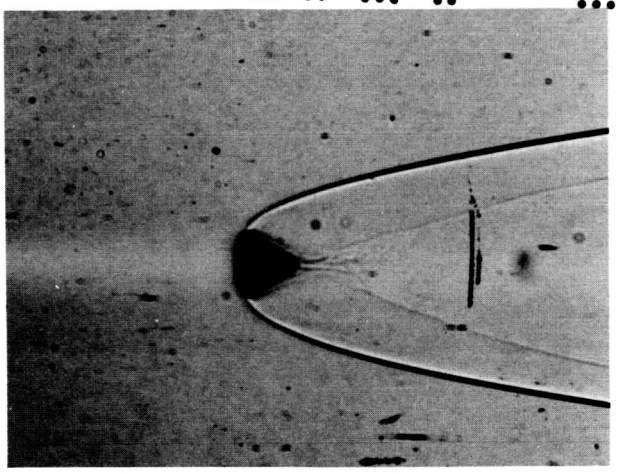

$V_\infty = 19{,}830$ fps

$M_\infty = 17.6$

$Re_D = 506{,}000$

$p_\infty = 100$ mm Hg

Figure 4.- Shadowgraph.

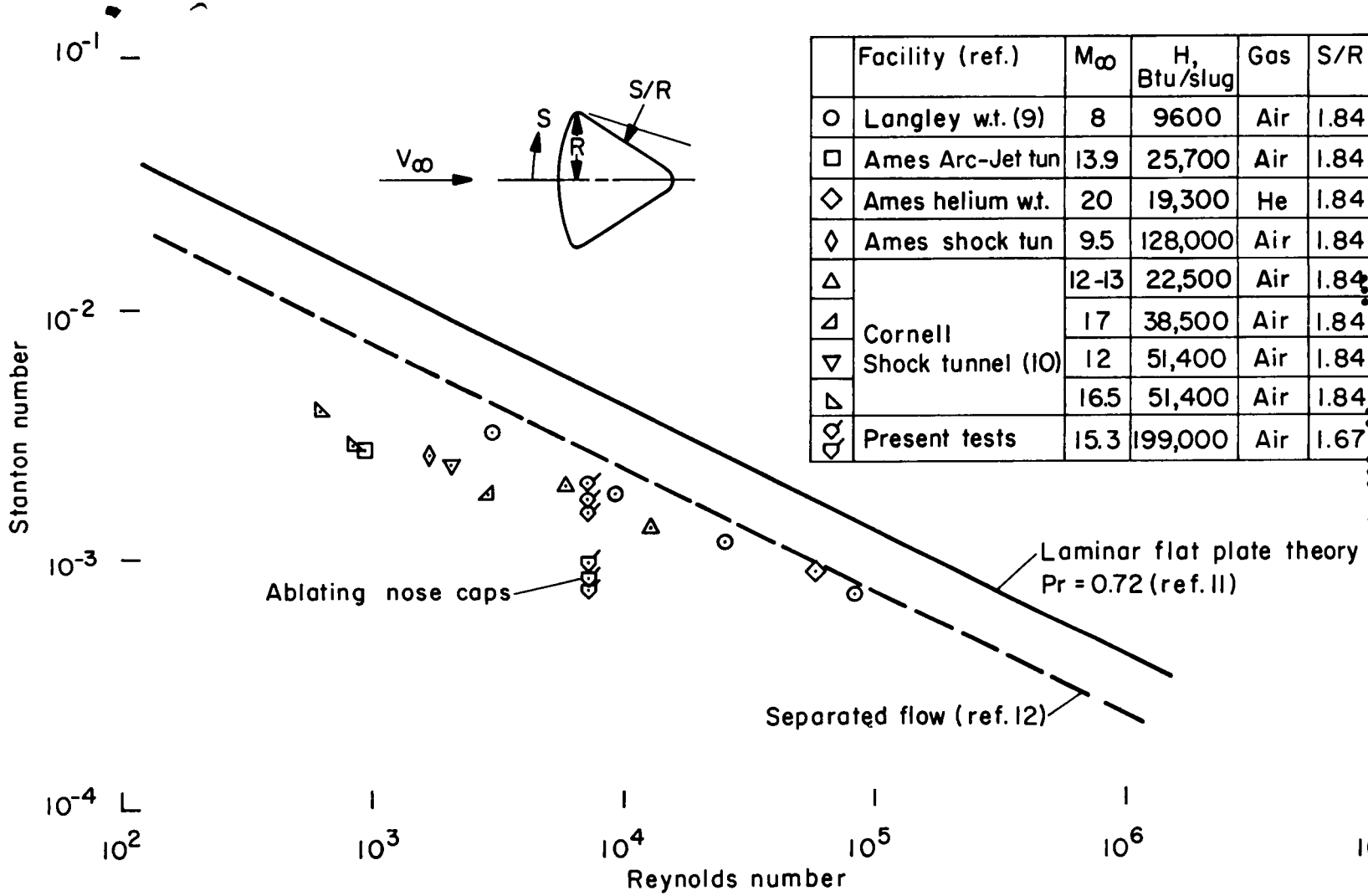

	Facility (ref.)	M_∞	H, Btu/slug	Gas	S/R
○	Langley w.t. (9)	8	9600	Air	1.84
□	Ames Arc-Jet tun	13.9	25,700	Air	1.84
◇	Ames helium w.t.	20	19,300	He	1.84
◊	Ames shock tun	9.5	128,000	Air	1.84
△	Cornell Shock tunnel (10)	12-13	22,500	Air	1.84
◿		17	38,500	Air	1.84
▽		12	51,400	Air	1.84
◺		16.5	51,400	Air	1.84
⊘	Present tests	15.3	199,000	Air	1.67

Figure 5.- Correlation of Apollo heat-transfer data at $\alpha = 0^{\circ}$.

NASA-Langley, 1965 A-2003